

Tuning TiO₂ Porosity of Multilayered Photoanode Towards Enhanced Performance of Dye Sensitized Solar Cell

Hashim Jabbar*, Basil A. Abdullah, Noor Ahmad

Department of Physics, College of Science, University of Basrah, Basrah, IRAQ.

*Correspondent contact: hashim.jabbar@uobasrah.edu.iq

Article Info

Received
16/07/2022

Accepted
06/09/2022

Published
30/12/2022

ABSTRACT

In this paper, we prepared Titanium Dioxide (TiO₂) based dye sensitized solar cells (DSSC). Downscaling of commercial TiO₂ powder have been achieved by systematic ball milling carried out using home-made ball milling device. Thin films were prepared and samples were characterized by XRD, SEM, UV-Vis and I-V. The main objective of this work is to prepare TiO₂ based (DSSC) using N3 dye and study the effect of the TiO₂ grain size inside the photoanode layer on the efficiency of the solar cell. UV-vis study of nanometer sized TiO₂ particles showed that the energy gap has shifted towards the lower wavelength in electromagnetic spectrum (blue shift), and then optical band gap is an indirect and allowed transition. Energy gap calculations of related grain size of showed quantum confinement effect. A sophisticated strategy for TiO₂ films consisting of tailoring monolayer, bilayer and trilayer of mixed multisized nanoparticles were adopted and investigated as DSSC electrodes. Our results showed that the dye sensitized solar cells can be substantially altered due to the designs and the particle size distributions of the TiO₂ photoelectrode. The maximum efficiency of 0.5% was reached by TiO₂ photoelectrode designed as a trilayer with a particles of wide size distribution from about 12 to 340 nm in the middle layer. The approach of light scattering in submicrometer-sized TiO₂ nanoparticles aggregates was adopted in order to interpret the enhancement of our DSSC efficiency over extending the length transported by electromagnetic wave hence to promote the light acquiring efficiency of photoelectrode thin film. The relatively larger particle sizes afford the TiO₂ films with both better packing and an increased capability for scattering of the incident electromagnetic wave, and hence improves our DSSC efficiency.

KEYWORDS: TiO₂ nanoparticles, ball milling, quantum confinement, DSSC.

INTRODUCTION

Since Gratzel's breakthrough discovery in 1991, (DSSCs) have emerged as an experimentally and commercially conclusive and alternative to traditional silicon-based photovoltaic devices. DSSCs are especially attractive because of their low cost, non-toxicity, ease of production and facile eco-friendly fabrication [1]. The current efficiency of DSSCs attained 13%, using Ru (II) dyes by improving substances and structure which kept its value less than the Si-based solar cells which gain efficiency of 20–30% [2-3]. Further improvement on (DSSCs) relies essentially on the better understanding of the energy conversion mechanisms, which is highly affected by the quality and design optimization of (DSSCs). Photoanode porosity in a (DSSC) can affect light

absorption and electron diffusion that govern the overall electrical current–voltage (I–V) characteristics. Thus, the cell performance can be optimized by improving the particle size distribution (porosity) of the cell electrode made up of small sized metal oxide powder, so that the adsorption of dye by the electrode could be increased and as a result, light harvesting efficiency (LHE) could also be increased [4-5]. Optimizing the porosity of photoelectrode increases the LHE by reducing the probability of optical reflection of the front surface, lengthening the optical path of the light through the cell, trapping a greater percentage of light within the thin active layers, and increasing the electrode's surface area. In addition, the quantum confinement effect can be observed when the size of the particle is too small to be comparable to the wavelength of the electron. confinement

effect changes the density of states and causes band gap/shift of band edges.

The aim of this work is utilizing light-scattering layer (LSL) effect which typically consists of large TiO₂ particles (340 nm), which are coated onto the bottom nanosized particles TiO₂, therefore, the incident sunlight reflects back to the dye adsorbed onto the TiO₂ film, increasing the light-absorbing capability of the dye.

MATERIALS AND METHODS

The commercially synthetic powders of Titanium Dioxide (Purity 99.7%) were purchased from Merck with average grain size about 340 nm. energy efficiency. Method of wet grinding have been chosen in this work due to some usefulness over dry grinding, for example, dry grinding consumes higher energy and produces wider particle size distributions compared with wet grinding. In addition, Surface roughness, particle agglomeration, magnitude of excess enthalpy, dust formation, and surface oxidation are higher in dry grinding than wet grinding. [6, 7, 8]. The milling processes have been carried out by mean of a home-made ball mill with some modifications developed regarding reducing of particle size. Time of grinding have been taken within the range between 2 to 8 h while the speed of rotation was kept constant at a calculated speed of 167 rpm for each experiment. All of our experiments were performed in a 160 mL stainless steel oval-shaped jar with 6 mm diameter stainless steel balls were used for these milling experiments. The grinding jar has been mounted horizontally, the direction of rotation of the grinding jar was vertical. A specific quantity of TiO₂ powder, distilled water and iron balls were weighted precisely and confined in the jar at laboratory temperature and atmospheric pressure. After this the jar closed tightly and subjected to rotation for grinding. Then after grinding, water was evaporated systematically in oven (50°C) for about 4 hours. The dried TiO₂ powder were smashed for 0.25 hour and examined. Measurements of Particle size distributions were performed using Zeta Nano Sizer at room temperature and the data was collected at scattering angle of 173°. Before the scanning, 1ml of nanosized particle suspensions for each specimen have been placed and enclosed inside a clean small plastic box to be measured. The dried nanopowders have been taken for SEM analysis. 50 k magnification and 100 nm at scale were used for

FESEM measurements. While for UV-vis measurements were carried out in the range of 200-1100 nm, P. TiO₂ Pastes have been manufactured using easy method: 6 g of dry TiO₂ powder was mixed with 0.03 L of deionized water and stirred using a programmed stirrer. To optimize the particles dispersal, we added to the mixture 1mL of nitric acid (70% concentration). The pastes then have been thickened by removing of surplus liquid under magnetic stirring at 80°C. The TiO₂ thin films have been synthesis using doctor blade a single layer of a prepared TiO₂ paste onto pre-cut (20 × 2.5 cm² pieces) transparent Fluorine doped Tin Oxide coated glass substrate. The thin films then were sintered in already heated oven at 623 °K for 30 min. Then the glass substrates have been cut into square area of (2 × 2 cm²) and anodes were designed into squares area of (1 × 1 cm²) by cracking the sides of the films using a microscopic tool. Film thickness and the roughness have been evaluated using stylus profilometer. Figure 1 shows a cartoon for TiO₂ films consisting of monolayer, bilayer and trilayer of mixed multisized nanoparticles.

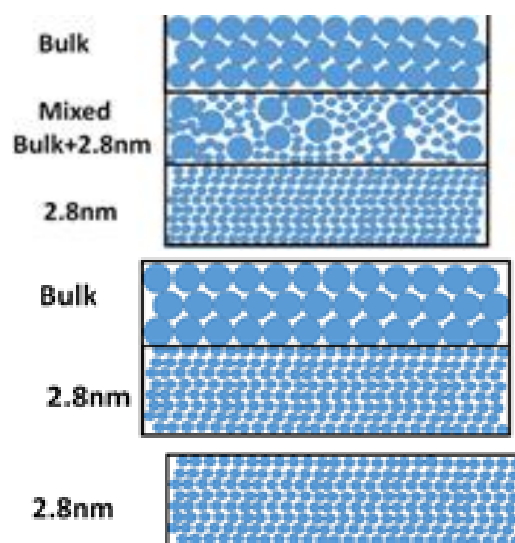


Figure 1. cartoon represents types of photoelectrode structures used in his study.

RESULTS AND DISCUSSION

Morphology of TiO₂ films

The contrast in the size, morphology of TiO₂ particles of the synthesized TiO₂ were examined by Field Emission Scanning Electron Microscopy (FESEM). TiO₂ particles of both bulk commercial and ball milled, demonstrate oval and spherical shape with clear boundary. Figure 2 shows SEM pictures of porous TiO₂ particles, for comparison we added the SEM images before and after

downscaling by ball milling. We used the image analysis program Image-J, by which a large number of particle diameters were calculated from the micrographs displayed and the size distribution histograms that accompany each image was obtained. The fitting of the histograms (continuous red line) for each size distribution was performed by a Log-Normal function from which the average value D of the distribution and the standard deviation σ were calculated. We can notice the huge difference between the size of particles after 8 hours of wet ball milling, the surface was very smooth and uniform over the large area.

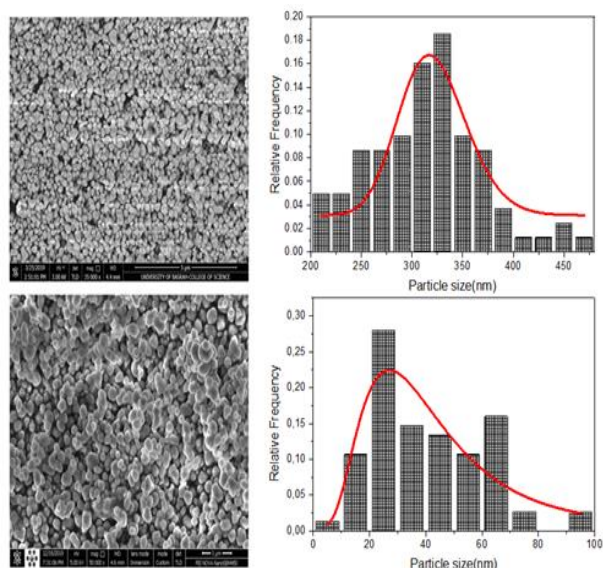


Figure 2. SEM photographs of porous TiO₂ films showing the surface morphology and nanoparticle size distribution before ball milling (top) and after 6 hours of ball milling (bottom).

Calculation of energy gap (E_g)

The variation of $(\alpha h\nu)^{1/2}$ as a function of $h\nu$ controls the values of the band gap energy E_g , by using Tauc formula [9]:

$$(\alpha h\nu) = B(h\nu - E_g)^m = f(h\nu) \quad (1)$$

In the above equation, B is a fixed value and m is a parameter relays on the kind of the transport between the valence band and the conduction band. The values of m is $1/2$ for a direct transport, 2 for an indirect transport. Regarding our TiO₂ samples that has an indirect band gap of 3.2 eV, hence $m = 2$. From the graph, showing $(\alpha h\nu)^{1/2}$ variation with $h\nu$, the band gap can be calculated by extrapolating the linear part of the curve to the zero ($\alpha = 0$) absorption as demonstrated in Figure 3. As can be seen In the Figure 3 that the E_g of TiO₂ layers increased as a particle size decreased from

3.12 to 3.41 eV. This can be explained by quantum confinement effect; the downscaled sample is relatively transparent and therefore has a wide E_g than the bulk non-milled sample. These band gap values are consistent with those found by other researchers and are very near to those of the Anatase phase of 3.2 eV [11].

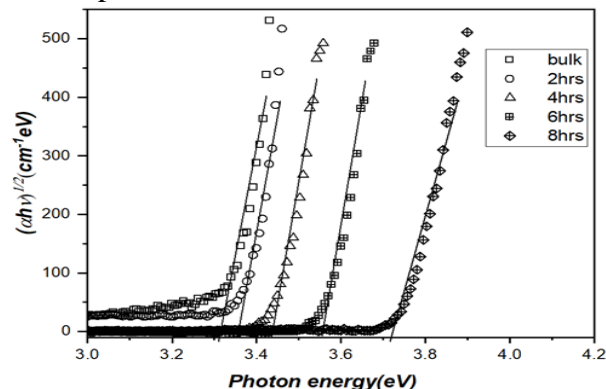


Figure 3. Tauc plot variation of $(\alpha h\nu)^2$ with photon energy for different milling times of TiO₂ thin film samples deposited on glass substrate.

The variation of the gap with regard to the grain size is presented in Figure 4 For sake of comparison, the theoretical curve of quantum confinement for the band gap are also presented in the same graph. The two curves agree well with each other exhibiting similar behavior with previous studies in confined shows the relation between the energy band gap of TiO₂ nanoparticles. It can be inferred that calculated energy gaps of different grain size TiO₂ nanoparticles distribute around the theoretical curve of quantum confinement could be written as [12]:

$$E_g = E_g^o + \frac{h^2\pi^2}{2d_g^2} \left[\frac{1}{m_e} + \frac{1}{m_h} \right] + d_g \left[p - \frac{1.8e^2}{\epsilon} \right] \quad (2)$$

Where E_g^o denotes the energy band gap of bulk material of large grain size ($d_g \rightarrow \infty$), m_e and m_h are the effective masses for the electron and hole, e is the electron charge ϵ is the dielectric constant, and p represents the polarizability term. Tables 1, 2, and 3 showed solar performance characteristics of the cells made from various TiO₂ photoanode designs with monolayer, bilayer, and trilayer. It can be inferred that the resistance of FTO conductive glasses after heating was enhanced to the value of $85 \sim 110 \Omega$. This is a reason

for a big influence on the performances of our DSSC solar cell since FTO utilized to transport electrons that are photo-generated from dye that adsorbed in TiO₂ films. For the Solar parameters from Table 3, it is very clear that the DSSC solar cell made from TiO₂ thin film produces the largest short-circuit current (J_{sc}). High photocurrent could be in general related to high porosity relevant to the surface area, which caused by an enhancement of the quantity of dye absorbed in the film bulk and visible light illumination intensity were fixed. In addition, this may cause by the existence of more anatase TiO₂, which promote the electron transportations [13,14]. The effect could be also interpreted by the larger TiO₂ particle size and increased surface area of photoelectrode as showed by SEM characterizations.

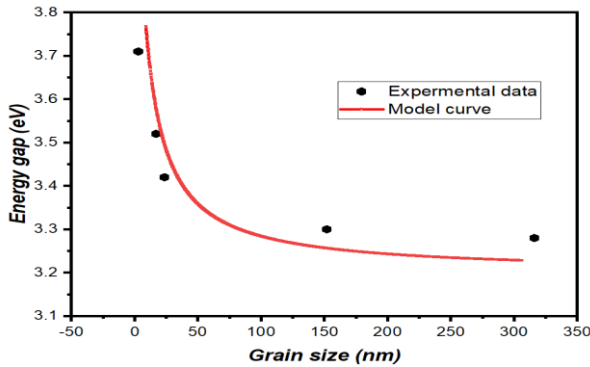


Figure 4. Energy gap (black dots) vs grain size for TiO₂ thin film samples deposited on glass substrate calculated using equation 1, and fitted (red line) by equation 2.

In Tanaka’s investigation, as the TiO₂ particle size increased, the possibility of the recombination of electron- and hole reduced [15,16]. The cell efficiency relies on the thickness of the TiO₂ film. For tackling this, trilayer TiO₂ thin film photoelectrode with a layer of 16 μm have been made. By utilizing this trilayer electrode in our DS solar cell, a photoconversion efficiency as high as 0.5% have been reached. The acceptable thickness of the film will build large particle pore size and satisfactory area which allow more redox electrolyte to adsorb through the film. Figure 5 represents the solar cell efficiency of DSSCs with milling time of monolayer, bilayer, and trilayer structures.

Table 1. Solar performance parameters of DSSCs with monolayer structure of different TiO₂ particle sizes in the bottom and top layers.

Milling time (h)	V _{oc} (mV)	J _{sc} (mA/cm ²)	P _{max} (mW)	F.F	η (%)	R _s (Ω)	R _{sh} (Ω)
0	399	1	5.10	0.32	0.2	8166	42985
2	163	0.8	2.03	0.41	0.12	2428	13355

4	465	0.75	4.37	0.34	0.3	12601	20325
6	394	0.75	5.25	0.44	0.32	6232	31654
8	525	0.9	6.83	0.41	0.47	5737	19281

Table 2. Solar performance parameters of DSSCs with bilayer structure of different TiO₂ particle sizes in the bottom and top layers.

Milling time (h)	V _{oc} (mV)	J _{sc} (mA/cm ²)	P _{max} (mW)	F.F	η (%)	R _s (Ω)	R _{sh} (Ω)
0	-	-	-	-	-	-	-
2	280	0.82	3.93	0.43	0.24	3668	15616
4	644	0.75	6.53	0.34	0.39	13517	38551
6	740	0.75	8.07	0.36	0.5	14106	47619
8	644	0.85	7.32	0.33	0.43	10650	30270

Table 3. Solar performance parameters of DSSCs with trilayer structure of different TiO₂ particle sizes in the bottom and top layers.

Milling time (h)	V _{oc} (mV)	J _{sc} (mA/cm ²)	P _{max} (mW)	F.F	η (%)	R _s (Ω)	R _{sh} (Ω)
0	-	-	-	-	-	-	-
2	284	1.03	5.04	0.43	0.3	3683	10444
4	670	0.75	7.85	0.39	0.47	12977	40571
6	525	1.0	7.59	0.36	0.45	9518	24125
8	736	0.75	8.30	0.37	0.5	15396	52777

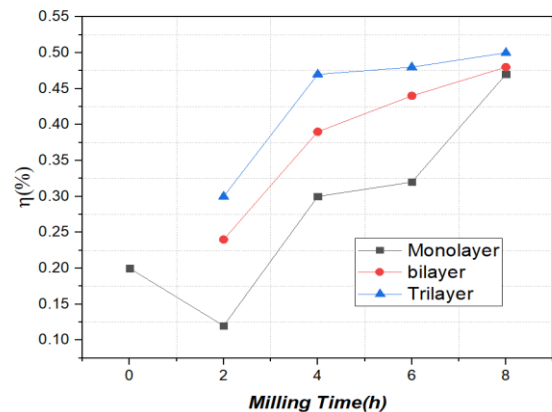


Figure 5. Solar cell efficiency of DSSCs with milling time of mono, bi, and trilayer structures.

CONCLUSIONS

In summary, ball mill technique enabled the fabrication of nanosized particles from commercially-available TiO₂ powders. Optical energy gap calculations of TiO₂ thin films of nanosized particles revealed quantum confinement effect. DSSC electrodes of TiO₂ films consisting monolayer, bilayer and trilayer of mixed different size- nanoparticles have been studied using N3 dye. Our results showed that the performance of the cells could be substantially altered by the designs and the size distributions of the TiO₂ photoelectrode. The best result of 0.5% efficiency was achieved using trilayer structure of photoelectrode with grain size range of (12nm-340nm). We conclude that the improved solar-cell performance of trilayer structure is caused by

increasing in the amount of dye absorbed in the bulk of the film, in addition of increasing of the distance transported by light which cause enhancement the electromagnetic wave yields of TiO₂ based photo-electrode film. The wide distribution of particle size offers the TiO₂ with either improved pressing and an increased capability for scattering of the incident electromagnetic wave, and hence enhances the DSSc efficiency.

ACKNOWLEDGEMENTS

Special thanks prof. M. A. Mahdi for invaluable collaboration in measurements and data collection at SEM Lab in Dept. of Physics, College of Science, Univ. of Basrah, and for asst. prof. F. A. Qasim who contributed with the necessary discussion and characterizations for the development of this paper, and the technical staff for technical support in the ball milling device.

Disclosure and conflict of interest: The authors declare that they have no conflicts of interest.

REFERENCES

- [1] O'Regan B, Gratzel M (1991) A low-cost, high-efficiency solar cell based on dye-sensitized colloidal TiO₂ films. *Nature* 353:737-740.
<https://doi.org/10.1038/353737a0>
- [2] S.Mathew, A. Yella, P. Gao et al., "Dye-sensitized solar cells with 13% efficiency achieved through the molecular engineering of porphyrin sensitizers," *Nature Chemistry*, vol. 6, no. 3, pp. 242- 247, 2014.
<https://doi.org/10.1038/nchem.1861>
- [3] Sayak Bhattacharya & Sajeev John "Beyond 30% Conversion Efficiency in Silicon Solar Cells: A Numerical Demonstration" *Nature Research Scientific Reports* 9:12482 (2019).
<https://doi.org/10.1038/s41598-019-48981-w>
- [4] F. Sauvage, D. Chen, P. Comte, F. Huang, L. P Heiniger., Y. B. Cheng, R. A. Caruso and M. Gratzel, *ACS Nano*, 2010, 4(8), 4420-4425.
<https://doi.org/10.1021/nn1010396>
- [5] T. K. Yun, S. S. Park, D. Kim, Y. K. Hwang, S. Huh, J. Y. Bae and Y. S. Won, *J. Power Sources*, 2011, 196(7),3678-3682.
<https://doi.org/10.1016/j.jpowsour.2010.11.162>
- [6] S. Chehreh Chelgani , M. Parian, P. Semsari Parapari, Y. Ghorbani, J. Rosenkranz "A comparative study on the effects of dry and wet grinding on mineral flotation separation-a review" *Elsevier Mater Res. Technol* 8(5) 5004-5011 (2019).
<https://doi.org/10.1016/j.jmrt.2019.07.053>
- [7] Chelgani, S. C., Parian, M., Parapari, P. S., Ghorbani, Y., & Rosenkranz, J. A comparative study on the effects of dry and wet grinding on mineral flotation separation - a review. *Integrative Medicine Research*, 8(5), 5004-5011 (2019).
<https://doi.org/10.1016/j.jmrt.2019.07.053>
- [8] Mill, E., & Ogonowski, Z. (2018). Comparison of Wet and Dry Grinding in, 1-19.
<https://doi.org/10.3390/min8040138>
- [9] Valenta, Jan Mirabella, Salvo SN - 978-981-4463-63-8 - Nanotechnology and Photovoltaic Devices: Light Energy Harvesting with Group IV Nanostructures (2015).
<https://doi.org/10.1201/b18090>
- [10] Munir H. Nayfeh *Fundamentals and Applications of Nano Silicon in Plasmonics and Fullerenes: Current and Future Trends (Micro and Nano Technologies)* Elsevier; 1st edition (2018).
- [11] Litter M. Heterogeneous photocatalysis transition metal ions in photocatalytic systems. *Appl Catal B: Environ* 1999; 23: 89-114.
[https://doi.org/10.1016/S0926-3373\(99\)00069-7](https://doi.org/10.1016/S0926-3373(99)00069-7)
- [12] T. Edvinsson, *Optical quantum confinement and photocatalytic properties in two-, one- and zero-dimensional nanostructures*, Royal Society (2018)
<https://doi.org/10.1098/rsos.180387>
- [13] N. G. Park, J. Van De Lagemaat, and A. J. Frank, "Comparison of dye-sensitized rutile-and anatase-based TiO solar cells," *Journal of Physical Chemistry*, vol. 104, no. 38, pp. 8989-8994, 2000.
<https://doi.org/10.1021/jp9943651>
- [14] Janczarek, M., & Kowalska, E. "On the Origin of Enhanced Photocatalytic Activity of Copper - Modified Titania in the Oxidative Reaction Systems". *JourCatalysts*, 7, 317; (2017).
<https://doi.org/10.3390/catal7110317>
- [15] Liu, Y., Lu, Y., Zeng, Y., Liao, C., Chung, J., & Wei, T. (2011)." Nanostructured Mesoporous Titanium Dioxide Thin Film Prepared by Sol-Gel Method for Dye-Sensitized Solar Cell", *International Journal of Photoenergy* Volume 2011, Article ID 619069 (2011).
<https://doi.org/10.1155/2011/619069>
- [16] K. Tanaka, M. F. V. Capule, and T. Hisanaga, "E ffect of crystallinity of TiO 2 on its photocatalytic action," *Chemical Physics Letters*, vol. 187, no. 1-2, pp. 73-76, 1991.
[https://doi.org/10.1016/0009-2614\(91\)90486-S](https://doi.org/10.1016/0009-2614(91)90486-S)

How to Cite

H. . Jabbar, B. A. Abdullah, and N. Ahmad, "Tuning TiO₂ Porosity of Multilayered Photoanode Towards Enhanced Performance of Dye Sensitized Solar Cell", *Al-Mustansiriyah Journal of Science*, vol. 33, no. 4, pp. 141–145, Dec. 2022.